Time-varying analysis of heart rate variability signals with Kalman smoother algorithm

Mika P Tarvainen‡, Stefanos D Georgiadis, Perttu O Ranta-aho and Pasi A Karjalainen

Department of Applied Physics, University of Kuopio, P.O. Box 1627, FIN-70211 Kuopio, Finland

E-mail: Mika.Tarvainen@uku.fi

Abstract. A time-varying parametric spectrum estimation method for analyzing nonstationary heart rate variability signals is presented. As a case study, the dynamics of heart rate variability during an orthostatic test is examined. In the method, the nonstationary signal is first modeled with a time-varying autoregressive model and the model parameters are estimated recursively with a Kalman smoother algorithm. The benefit of using Kalman smoother is that the lag error present in Kalman filter, as well as in all other adaptive filters, can be avoided. The spectrum estimates for each time instant are then obtained from the estimated model parameters. Statistics of the obtained spectrum estimates are derived using the error propagation principle. The obtained spectrum estimates can further be decomposed into separate components and, thus, the time-variation of low and high frequency components of heart rate variability can be examined separately.

Keywords: heart rate variability, Kalman smoother, time-varying spectrum estimation, error propagation, spectral decomposition

1. Introduction

The variation of the heart beat interval or heart rate variability (HRV) is a consequence of the autonomic nervous system control of the heart. Both the sympathetic and parasympathetic branches are effective. Roughly speaking, sympathetic activity tends to increase heart rate (HR↑) and parasympathetic tends to decrease it (HR↓) (Berntson *et al* 1997). Sympathetic innervation covers also arterial walls and causes vasoconstriction. In addition to central control, there are some feedback mechanisms such as the arterial baroreceptors that can provide quick reflexes to heart rate.

The most conspicuous periodic component of HRV is the respiratory sinus arrhythmia (RSA) which is considered to range from 0.15 to 0.4 Hz. In addition to the physiological influence of breathing on HRV, this high frequency (HF) component is generally believed to be of parasympathetic origin. Another widely studied component of HRV is the low frequency (LF) component ranging form 0.04 to 0.15 Hz. The rhythms within the LF band are nowadays generally thought of being both of sympathetic and parasympathetic origin (Berntson *et al* 1997). Thus, HRV is

‡ All correspondence to Mika P Tarvainen, Department of Applied Physics, University of Kuopio, P.O.Box 1627, FIN-70211 Kuopio, Finland, phone: +358-17-162369, fax: +358-17-162373, e-mail: Mika.Tarvainen@uku.fi

commonly examined through spectral analysis and, e.g., the LF/HF ratio is considered as an index of sympatho-vagal balance.

Due to the complex control systems of HRV, it is presumable that the characteristics of HRV (e.g. the powers and frequencies of LF and HF components) vary in time. Especially, changes in physiological conditions may produce significant such variations. For example, in the orthostatic test, subject stands up after lying supine for few minutes. After standing up, HR starts to increase to compensate the decrease in blood pressure. On supine, the high frequency variation of HR is typically strong, often higher than the low frequency variation. At the instant of standing, an immediate strong decrease in HF variation and a more gradual increase in LF variation has been observed (Keselbrener and Akselrod 1996). In order to analyze such changes, time-frequency methods are required.

During the last decade, various such methods have been applied for HRV analysis. The applied time-frequency methods include short time Fourier transformation (STFT) and wavelet transform (Keselbrener and Akselrod 1996, Wiklund *et al* 1997), time-frequency distributions such as the Wigner distribution (Novak and Novak 1993, Pola *et al* 1996, Vila *et al* 1997, Mainardi and Cerutti 2004), and time-varying autoregressive (AR) modeling based methods (Bianchi *et al* 1993, Bianchi *et al* 1997). The benefit of AR methods over the other methods is that AR spectrum estimates can be decomposed into separate spectral components.

In this paper, we present a Kalman smoother method for estimating time-varying characteristics of HRV. In the method, the HRV signal is first modeled as an output of time-varying AR model. The time-varying model parameters are estimated recursively with a Kalman smoother algorithm. By using Kalman smoother, the lag error present in all adaptive filters such as Kalman filter, least mean square (LMS) or recursive least squares (RLS) can be avoided. Also the error covariance for the AR parameter estimates is evaluated iteratively in the Kalman smoother algorithm. The time-varying spectrum estimate is obtained from the estimated model parameters and its statistics can be evaluated by using the error propagation formula as derived in this paper. The time-varying spectrum can be further decomposed into separate spectral components. This is especially advantageous in HRV applications, where LF and HF components are generally aimed to be distinguished.

2. Methods

The formulation of the Kalman smoother equations is based on *state-space formalism*. In this paper, the HRV dynamics are estimated using a time-varying AR model of order p given by

$$x_t = -\sum_{j=1}^{p} a_t^{(j)} x_{t-j} + e_t \tag{1}$$

where $a_t^{(j)}$ is the value of the j'th AR parameter at time t and e_t is the observation error. By denoting

$$H_t = (x_{t-1}, \ldots, x_{t-p}) \tag{2}$$

$$\theta_t = (-a_t^{(1)}, \ldots, -a_t^{(p)})^T \tag{3}$$

the time-varying AR model can be written in the form

$$x_t = H_t \theta_t + e_t \tag{4}$$

which is a linear observation model with H_t being the regression vector. The evolution of the state (i.e. the AR parameters) θ_t when no prior information is available is typically described with the random walk model

$$\theta_{t+1} = \theta_t + w_t \tag{5}$$

where w_t is the state noise term. Equations (4) and (5) form the state-space signal model for the time-varying AR process x_t and the evolution of the AR parameters can now be estimated using the Kalman smoother algorithm.

2.1. Kalman smoother algorithm

The Kalman smoother algorithm presented in this paper consists of a Kalman filter algorithm and a fixed-interval smoother. The Kalman filter is a real time processing algorithm in which the state estimate is updated immediately after a new observation is available. The fixed-interval smoother, on the other hand, estimates each state θ_t based on all the observations and, thus, the estimates are expected to be more accurate than the filter estimates.

The Kalman filtering problem is to find the linear mean square estimator $\hat{\theta}_t$ for state θ_t given the observations $x_1, x_2, \ldots, x_t$. The observation and state noise processes e_t and w_t are assumed to be uncorrelated zero-mean random processes (white noise processes) with covariances C_{e_t} and C_{w_t}. For the derivation of the Kalman filter equations see, e.g., (Melsa and Cohn 1978). For the time-varying AR model case, these equations can be written in the form

$$C_{\tilde{\theta}_{t|t-1}} = C_{\tilde{\theta}_{t-1}} + C_{w_{t-1}} \tag{6}$$

$$K_t = C_{\tilde{\theta}_{t|t-1}} H_t^T (H_t C_{\tilde{\theta}_{t|t-1}} H_t^T + C_{e_t})^{-1} \tag{7}$$

$$\hat{\theta}_t = \hat{\theta}_{t-1} + K_t(x_t - H_t\hat{\theta}_{t-1}) \tag{8}$$

$$C_{\tilde{\theta}_t} = (I - K_t H_t) C_{\tilde{\theta}_{t|t-1}} \tag{9}$$

where $\tilde{\theta}_t$ is the state estimation error $\tilde{\theta}_t = \theta_t - \hat{\theta}_t$, $\tilde{\theta}_{t|t-1}$ is the state prediction error $\tilde{\theta}_{t|t-1} = \theta_t - \hat{\theta}_{t-1}$, and K_t is the Kalman gain vector. The Kalman filter equations given above can be considered as the generalized form of an adaptive filter. In fact, several other adaptive filters such as LMS or RLS can be derived from Kalman filter equations with specific assumptions.

The fixed-interval smoothing problem is to find estimates $\hat{\theta}_t^{\mathrm{S}}$ for each state θ_t given all the observations $x_1, x_2, \ldots, x_N$. The superscript S is used here to refer to smoothed estimates. Different approaches for the derivation of the fixed-interval smoothing equations have been presented. Here, the so-called *Rauch-Tung-Striebel* form (Rauch *et al* 1965) of the smoothing equations is adopted. In this approach, the Kalman filter estimates $\hat{\theta}_t$ are assumed to be already determined and the smoothed estimates are obtained by running the filtered estimates backwards in time by taking $t = N-1, N-2, \ldots, 1$. The smoothing recursions for the state estimate and error covariance are then given by

$$\hat{\theta}_t^{\mathrm{S}} = \hat{\theta}_t + A_t(\hat{\theta}_{t+1}^{\mathrm{S}} - \hat{\theta}_t) \tag{10}$$

$$C_{\tilde{\theta}_t^{\mathrm{S}}} = C_{\tilde{\theta}_t} + A_t(C_{\tilde{\theta}_{t+1}^{\mathrm{S}}} - C_{\tilde{\theta}_{t+1|t}})A_t^T \tag{11}$$

$$A_t = C_{\tilde{\theta}_t} C^{-1}_{\tilde{\theta}_{t+1|t}} \tag{12}$$

where the filtered estimates are used for the initialization, i.e. $\hat{\theta}_N^{\mathrm{S}} = \hat{\theta}_N$ and $C_{\tilde{\theta}_N^{\mathrm{S}}} = C_{\tilde{\theta}_N}$.

2.2. Initialization of the algorithm

First of all, it should be noted that the smoother algorithm does not require any additional specifications, but the ones adopted for the filter algorithm act on the smoothed estimates as well. Thus, only the initialization and operation of the Kalman filter algorithm need to be considered.

To operate the Kalman filter algorithm, both the initial values for the state estimate $\hat{\theta}_t$ and its error covariance $C_{\tilde{\theta}_t}$ and the noise covariances C_{w_t} and C_{e_t} need to be specified. In practice, the distribution of the initial state θ_0 is unknown and, therefore, the initial values $\hat{\theta}_0$ and $C_{\tilde{\theta}_0}$ are usually determined by some conventional means. A common approach for the initialization is to set the initial state estimate, e.g., to $\hat{\theta}_0 = 0$ and its error covariance, e.g., to $C_{\tilde{\theta}_0} = I$ and then to run a short segment from the beginning of data backwards in time. If the initial guess for the error covariance is far from the true one, then the error covariance does not necessarily have enough time to converge on the true value. In this case, the backward run may be repeated until a convergence is observed. The values obtained for the state estimate and error covariance in the backward run are then used as initial values in the forward run. This kind of initialization is not, however, needed if sufficient amount of data before the time instant of interest is available.

The state noise covariance C_{w_t} and the observation noise covariance C_{e_t} are the terms that determine the adaptation of the Kalman filter (i.e. the speed of change of the state estimate) through the Kalman gain vector K_t. In (Isaksson and Wennberg 1976), $C_{w_t} = \sigma_w^2 I$ and $C_{e_t} = \sigma_e^2 = 1$, where σ_w^2 is the state noise covariance coefficient, I is a $p \times p$ identity matrix, and σ_e^2 the observation noise variance, were used. In this case, however, the observation noise variance has no relation to the true error variance and, thus, the state estimates may become meaningless. In this paper, we have estimated the observation noise variance iteratively at every step of the Kalman filter equations as

$$\hat{\sigma}_{e_t}^2 = \gamma\, \hat{\sigma}_{e_{t-1}}^2 + (1-\gamma)\, \epsilon_t^2 \tag{13}$$

where $\gamma < 1$ is an adaptation coefficient (here $\gamma = 0.95$ was used) and ϵ_t is the one step prediction error

$$\epsilon_t = x_t - H_t \hat{\theta}_{t-1}. \tag{14}$$

A similar approach for the observation error variance estimation was adopted at least in (Schack *et al* 1995). The state noise covariance, on the other hand, is selected to be diagonal as in (Isaksson and Wennberg 1976) and the covariance coefficient σ_w^2 is adjusted at every step of the Kalman filter equations as

$$\hat{\sigma}_{w_t}^2 = \mathrm{UC}\, \hat{\sigma}_{e_t}^2 / \hat{\sigma}_{x_t}^2 I \tag{15}$$

where $\hat{\sigma}_{x_t}^2$ is the estimated variance of the observed HRV signal at time t and UC is an update coefficient through which the adaptation of the algorithm can be adjusted. The observation variance is included in order to remove the influence of signal amplitude on the estimates (Bohlin 1977). This way, the update coefficient does not need to be selected separately for HRV signals with different variability levels. The adaptation of the algorithm can be increased by increasing UC. The variance of the state estimates is, however, inversely proportional to the value of UC and, therefore, UC should be specified in such a way that a desired balance between the filter adaptation and estimate variance is obtained.

2.3. Time-varying spectrum estimation

The time-varying spectrum estimate is obtained from the momentary AR parameter estimates $\hat{a}_t^{(j)}$ as

$$P_t(f) = \frac{\hat{\sigma}_e^2/f_s}{|1 + \sum_{j=1}^{p} \hat{a}_t^{(j)} e^{-i2\pi jf/f_s}|^2} \tag{16}$$

where f_s is the sampling frequency, $\hat{a}_t^{(j)}$ is the AR parameter estimate at time t, and $\hat{\sigma}_e^2$ is the variance of the estimated observation error process (i.e. the variance of $\hat{e}_t = x_t - H_t\hat{\theta}_t^{\mathrm{S}}$).

Note that equation (16) is a continuous function of frequency and can, thus, be evaluated at any desired frequencies up to the Nyquist frequency $f_s/2$. However, the frequency resolution is naturally not infinite, but is determined by the underlying parameter model, i.e. the model structure and model order. When compared to classical FFT based spectrum estimation methods, the resolution of parametric methods is higher due to the implicit extrapolation of the autocorrelation sequence (Marple 1987).

The characteristics of the Kalman smoother spectrum depend strongly on the order of the AR model. As a rule of thumb it can be said that a smaller model order results in a smoother spectrum and a selection of too high a model order can produce spurious peaks in the spectrum, but in any case the order should be at least twice the number of expected peaks in the spectrum. The selection of the model order in time-varying case is not a straightforward problem, but there have been some attempts, e.g., in (Goto *et al* 1995, Haseyama and Kitajima 2001). In stationary case, on the other hand, there exist simple criteria such as the final prediction error (FPE), Akaike's information criterion (AIC), and minimum prediction length (MDL) (Akaike 1969, Akaike 1974, Rissanen 1983). These, as well as all the other such criteria, are, however, designed for true AR processes and yield, therefore, more or less biased results for real life signals.

2.4. Statistics of Kalman smoother spectrum estimates

The covariance matrix of the state estimation error $\tilde{\theta}_t$ is calculated iteratively at every step of the Kalman smoother algorithm in (11), thus providing a statistical measure of the uncertainty in $\hat{\theta}_t$. That is, the error variance and covariance of the AR parameter estimates (the state estimate) at each time t are known and the error variance of the spectrum estimate at time t can be evaluated by using the error propagation formula

$$\begin{aligned}\sigma^2_{P_t(f)} = &\sum_{k=1}^{p} \left(\frac{\partial P_t(f)}{\partial \hat{a}_t^{(k)}} \right)^2 \sigma^2_{\hat{a}_t^{(k)}} \\ &+ \sum_{k=1}^{p} \sum_{\substack{l=1 \\ l \neq k}}^{p} \frac{\partial P_t(f)}{\partial \hat{a}_t^{(k)}} \frac{\partial P_t(f)}{\partial \hat{a}_t^{(l)}} \sigma_{\hat{a}_t^{(k)} \hat{a}_t^{(l)}}\end{aligned} \tag{17}$$

where $\sigma^2_{\hat{a}_t^{(k)}}$ is the error variance of the k'th AR parameter estimate, $\sigma_{\hat{a}_t^{(k)} \hat{a}_t^{(l)}}$ is the error covariance of k'th and l'th AR parameter estimates, and the partial derivative

of $P_t(f)$ with respect to $\hat{a}_t^{(k)}$ can be written in the form

$$\frac{\partial P_t(f)}{\partial \hat{a}_t^{(k)}} = \frac{-2\hat{\sigma}_e^2/f_s \left(\cos k\omega + \sum_{j=1}^p \hat{a}_t^{(j)} \cos(j-k)\omega\right)}{\left[(1+\sum_{j=1}^p \hat{a}_t^{(j)} \cos j\omega)^2 + (\sum_{j=1}^p \hat{a}_t^{(j)} \sin j\omega)^2\right]^2} \tag{18}$$

where $\omega = 2\pi f/f_s$.

The further calculation of power and corresponding error variance for a specific band is straightforward. If the power spectrum is evaluated at discrete frequencies f_j then, for example, the power of the LF band at time t is obtained as

$$P_t^{\mathrm{LF}} = \sum_{f_j \in \mathrm{LF\ band}} P_t(f_j)\,\Delta f \tag{19}$$

where Δf is the frequency grid interval $\Delta f = f_j - f_{j-1}$. The partial derivative of the band power with respect to $P_t(f_j)$ is Δf and, thus, the error variance of the band power is obtained as

$$\sigma^2_{P_t^{\mathrm{LF}}} = \sum_{f_j \in \mathrm{LF\ band}} \Delta f^2 \sigma^2_{P_t(f_j)} \tag{20}$$

where the power values at different frequencies are treated as uncorrelated. Similarly, the power and its error variance could be calculated for the HF band and, furthermore, error variance could be derived for LF/HF ratio.

2.5. Spectral decomposition

One property of the AR spectrum estimation methods, that is especially advantageous in HRV applications, is that the spectrum can be divided into separate components as follows. Equation (16) can also be written in the factored form

$$P_t(f) = \frac{\hat{\sigma}_e^2/f_s}{\prod_{j=1}^p (z - \alpha_t^{(j)})(1/z - \alpha_t^{(j)*})} \tag{21}$$

where $z = e^{i2\pi f/f_s}$, $\alpha_t^{(j)}$ are the time-varying roots of the AR polynomial (also called poles), and * denotes complex conjugate. Now, consider a pole $\alpha_t^{(j)}$ positioned at frequency f_j. The spectrum of this single component in the vicinity of f_j can be estimated as

$$P_t^{(j)}(f) \approx \frac{c_t^{(j)}}{(z - \alpha_t^{(j)})(1/z - \alpha_t^{(j)*})}, \quad z = e^{i2\pi f/f_s} \tag{22}$$

where the constant $c_t^{(j)}$ is given by

$$c_t^{(j)} \approx \frac{\hat{\sigma}_e^2/f_s}{\prod_{\substack{k=1 \\ k\neq j}}^p (z - \alpha_t^{(k)})(1/z - \alpha_t^{(k)*})}, \quad z = e^{i2\pi f_j/f_s}. \tag{23}$$

That is, the part $c_t^{(j)}$ of the AR spectrum estimate is assumed to be constant when $f \approx f_j$. The sum of the component spectra is approximately equal to the AR spectrum estimate, i.e. $P_t(f) \approx \sum_{j=1}^p P_t^{(j)}(f)$.

The powers of the components can be estimated, e.g., by using the method proposed in (Johnsen and Andersen 1978). In this approach, the power of the component positioned at frequency f_j is estimated with the residue

$$P_t^{f_j} = d\,\mathrm{Re}\left\{\mathrm{Res}\left\{\frac{P_t(z)}{z}\right\}\Big|_{z=e^{i2\pi f_j/f_s}}\right\} \tag{24}$$

where the residue is evaluated at $z = e^{i2\pi f_j/f_s}$ and the coefficient $d = 1$ for real poles and $d = 2$ for complex poles. The previous equation can be solved by evaluating

$$P_t^{f_j} = d\,\mathrm{Re}\left\{\frac{\hat{\sigma}_e^2(z-\alpha_t^{(j)})}{zA(z)A(1/z)}\right\} \tag{25}$$

where $A(z) = \prod_{k=1}^{p}(z-\alpha_t^{(k)})$ and $A(1/z) = \prod_{k=1}^{p}(1/z-\alpha_t^{(k)*})$, at $z = \alpha_t^{(j)}$ (Marple 1987). This method for component power estimation works for well-separated poles, but for poles close to each other power estimates can yield even negative values. A more robust way to estimate the powers is, however, to simply calculate the areas of the spectral components.

3. ECG measurements and preprocessing

ECG measurements were made from five healthy young male subjects. As an experimental protocol, an orthostatic test including a 30 second breath hold at the end was performed. In the experiment, the subject first lay supine for over five minutes and then stood up. After standing of about five minutes the subject held his breath for 30 seconds. The ECG signal was measured using a Neuroscan system (Compumedics Limited) with the new SynAmps^2 amplifier. ECG electrodes were placed according to the conventional 12 lead system with the Mason-Likar modification. For analysis, the lead II was chosen for each subject. The sampling rate of the ECG signal was 1000 Hz. The QRS fiducial points were then extracted from the ECG signal by using an adaptive QRS detection algorithm and the RR interval series was formed. The RR interval series was further transformed to evenly sampled time series by using a 4 Hz cubic spline interpolation.

4. Results

In adaptive filters such as Kalman filter, LMS, or RLS the parameters at a specific time instant are always estimated based on the past observations, i.e. there is no knowledge of the current or future observations. Understandably, this creates a tracking lag in the parameter estimates. In the Kalman smoother, on the other hand, the parameters at a specific time instant are estimated based on all the observations (past and future) and, thus, the lag error can be avoided. This benefit of Kalman smoother was already addressed in (Tarvainen *et al* 2004), where Kalman smoother was compared to LMS and RLS algorithms and also to the commonly used spectrogram method. Furthermore in (Tarvainen *et al* 2004), the performance of Kalman smoother was tested with simulations and it was applied to the estimation of nonstationary electroencephalograms. The observed benefits of the Kalman smoother were the elimination of the lag error and the high quality time-frequency resolution. Here, we will start by applying the Kalman smoother method to the RR interval series of one of the measured subjects. Results for rest of the subjects will be presented at the end.

The obtained RR interval series for subject 1 is presented on top of figure 1. The time instant of standing up and the breath hold period are indicated on top. The low frequency trend components of HRV can distort the AR spectrum estimate as was shown in (Tarvainen *et al* 2002). Thus, the trend was removed by using a smoothness priors based method described in (Tarvainen *et al* 2002). The estimated trend is

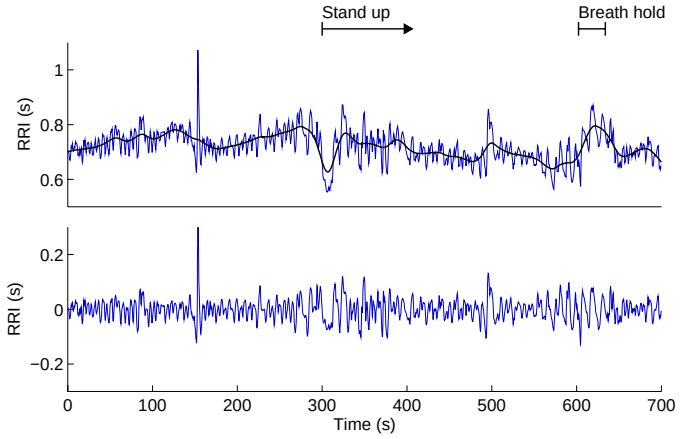

Figure 1. An orthostatic test recording with a 30 second breath hold at the end: the RR interval series with the estimated trend (top) and the detrended RR interval series (bottom).

presented with bold line on top and the detrended RR interval series on bottom of figure 1. The changes between the HF and LF variability due to the posture change at about 300 seconds are evident. In addition, a decrease in HR is observed for the breath holding.

The first decision in the use of the Kalman smoother spectrum estimation method is the selection of the AR model order. Here the model order was selected based on three different model order selection criteria, i.e. FPE, AIC, and MDL. Each criterion was evaluated separately for supine and standing periods. All these criteria are functions of model order and the corresponding prediction error variance. For the estimation of the prediction error variance a forward-backward least squares method, also known as the modified covariance method (Marple 1987), was applied. The FPE, AIC, and MDL criteria as functions of model order p for supine and standing periods for subject 1 are presented in figure 2 (a).

According to the model order selection criteria, the "optimal" model order for subject 1 seemed to be a bit higher for the standing period than for the supine period. For some subjects, the situation was however the opposite. As a good compromise for all subjects a model order $p = 16$ [indicated with vertical lines in figure 2 (a)] was selected for the analysis. The stationary AR spectrum estimates for the selected model order are presented on top of figure 2 (b). For comparison the spectrum estimates were also calculated with the Welch's periodogram method, shown on bottom of figure 2 (b).

The Kalman smoother spectrum estimate was then calculated using the time-varying AR(16) model for the RR interval series. The detrended RR interval series and the corresponding Kalman smoother spectrum for subject 1 are presented in figure 3. The update coefficient UC of the Kalman smoother algorithm was set to $1 \cdot 10^{-5}$. The decision of UC was made as a compromise between the adaptation speed of the algorithm and the statistics of the resulting spectrum estimate. The variance of the Kalman smoother spectrum estimates was evaluated according to (17) and (18). Kalman smoother spectrum estimates with $\pm$2SD intervals for two selected time instants ($t = 200$ and $t = 400$ seconds) are presented in figure 4.

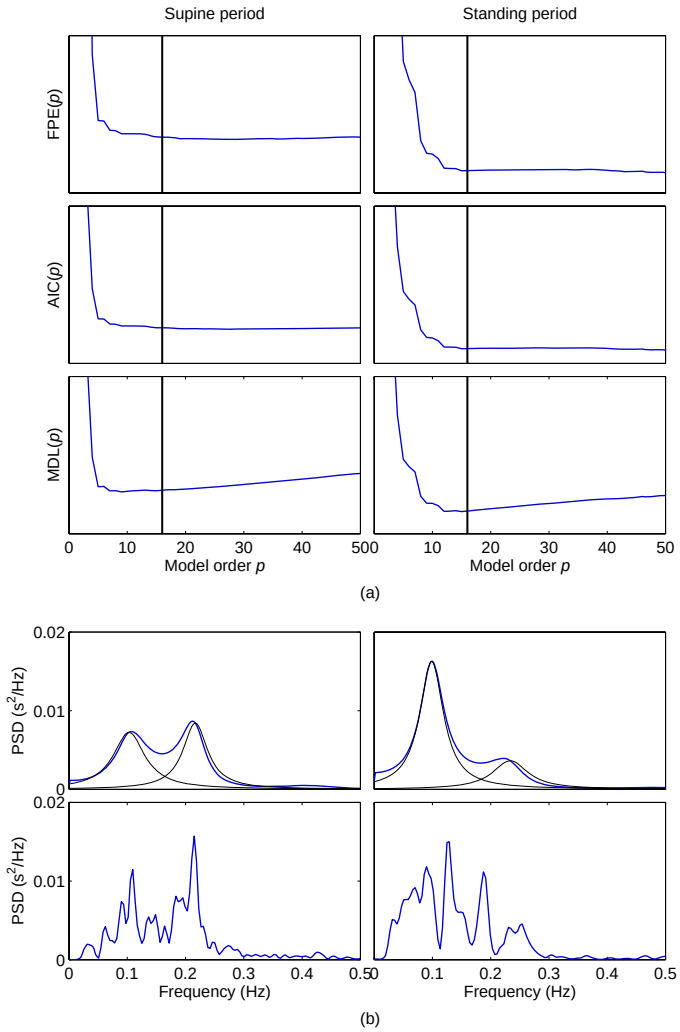

Figure 2. Selection of the AR model order. (a) FPE, AIC, and MDL criteria as functions of model order p for supine (left) and standing (right) periods. The selected model order $p = 16$ is indicated with vertical lines. (b) The AR spectrum for the selected order $p = 16$ (top) compared to Welch's periodogram (bottom) for supine (left) and standing (right) periods.

The LF and HF band powers and the LF/HF ratio as functions of time were then calculated. The band powers are simply obtained by integrating the spectrum over the specific frequency band according to (19). The variances of the band powers were calculated according to (20) and the variance of the LF/HF ratio correspondingly by using the error propagation formula. The obtained band powers and LF/HF ratio with ± 2SD intervals are presented in figure 5.

Finally, we utilize spectral decomposition to divide the Kalman smoother spectrum into separate LF and HF components. The spectral components are extracted by using (22) and (23). The obtained LF and HF components are presented in figure 6. The decomposition of the spectra at $t = 200$ and $t = 400$ seconds is

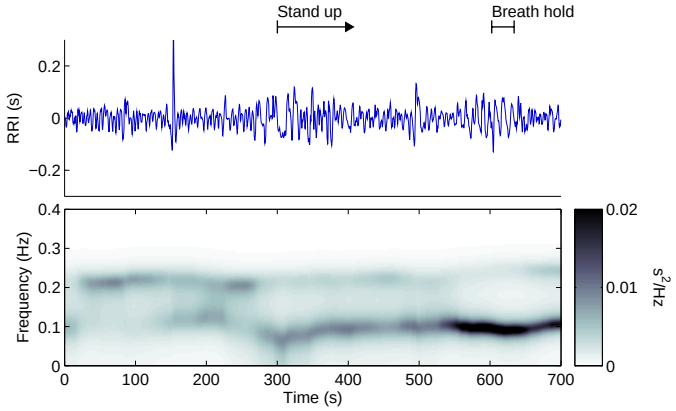

Figure 3. Time-varying spectrum estimation of HRV. The detrended RR interval series (top) and the corresponding Kalman smoother spectrum estimate (bottom).

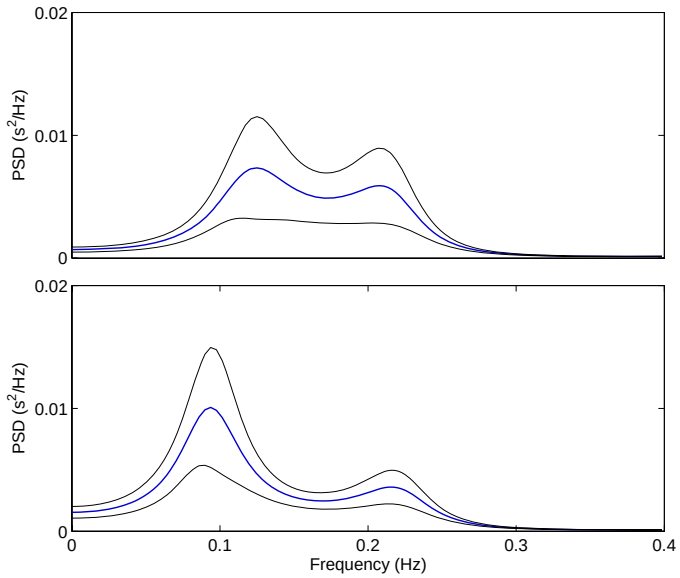

Figure 4. Kalman smoother spectrum estimates (—) at times $t = 200$ s (top) and $t = 400$ s (bottom) with the $\pm$2SD intervals (—).

illustrated on top of the figure. The powers of the LF and HF components can be evaluated simply by calculating the areas of the spectral components or by using the residue method [equations (24) and (25)]. The component power estimates using the two different methods are presented in figure 7 with comparison to the corresponding band powers already presented in figure 5. The HF component powers are quite close to the corresponding band power, but the LF component powers are noticeably higher than the corresponding band power.

The HRV data of the four other subjects were analyzed accordingly with the Kalman smoother method. The RR interval series of different subjects were clearly distinct from each others. The overall intensity of the variability as well as the LF/HF

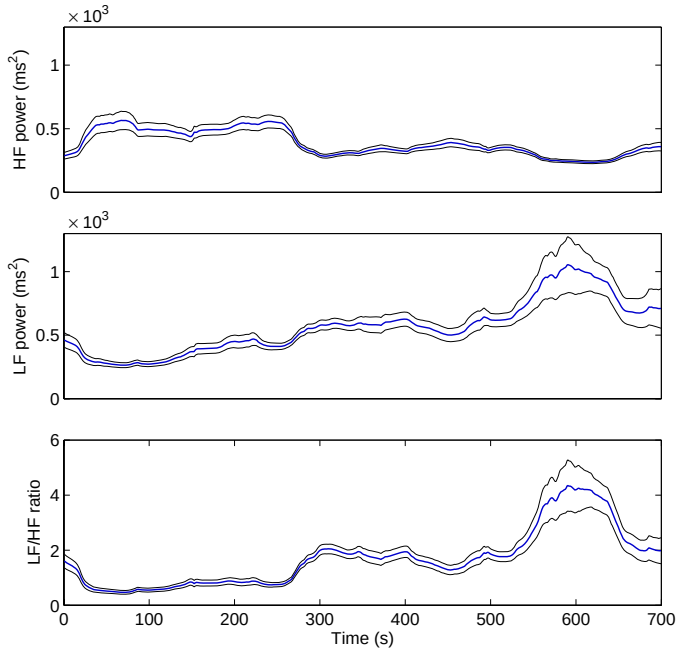

Figure 5. Estimated dynamics of LF and HF band powers and LF/HF ratio (—) with ±2SD intervals (—).

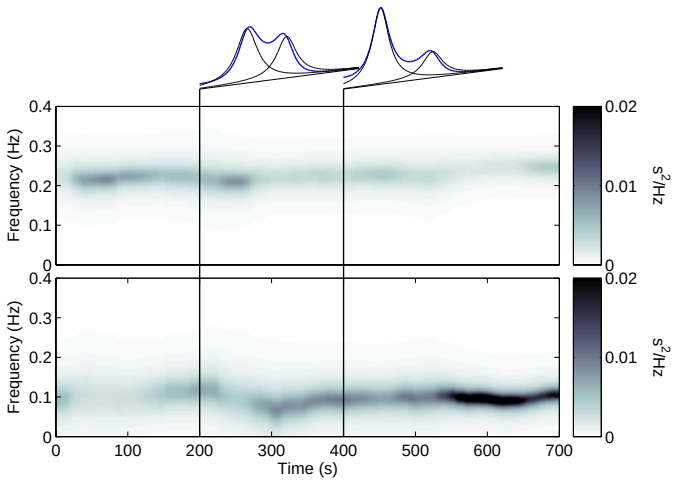

Figure 6. Decomposition of the Kalman smoother spectrum into LF (bottom) and HF (top) spectral components.

dynamics varied between subjects. The RR interval series and the Kalman smoother estimates for subjects 2–5 are presented in figures 8 (a), (b), (c), and (d). The RR interval series and the estimated trends are presented on top of each subfigure and the Kalman smoother spectrum estimates on the middle. The LF and HF component powers obtained using the two different methods and the corresponding band powers

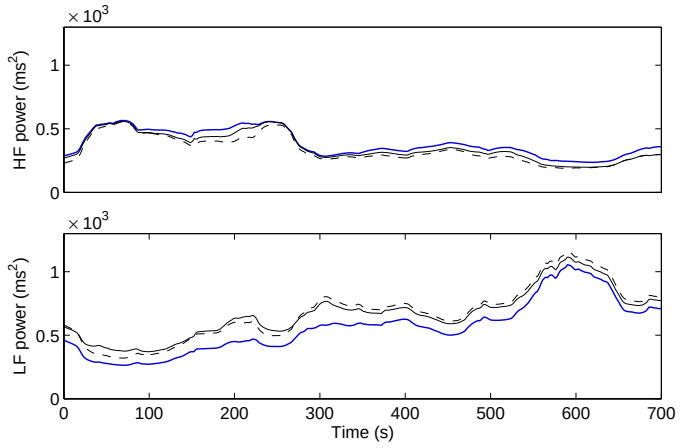

Figure 7. LF and HF component powers as band powers from non-decomposed spectrum (—), areas of corresponding decomposed spectral components (—), and by using the residue method (– – –).

are presented on bottom of each subfigure. Problems in component power estimation arise when the separation of the LF and HF components is not clear [see figures 8 (a) and (d)]. For example, in figure 8 (d), the evolution of the strongest power component between the LF and HF bands results in drastic changes in component power estimates. The break in the LF component power estimates indicates that none of the AR model roots were temporarily positioned within the LF band.

5. Discussion

A Kalman smoother spectrum estimation method for time-varying estimation of HRV dynamics was presented. Kalman smoother is theoretically an optimal linear mean square estimator of the AR parameters and, thus, the method is statistically favorable. In addition, the frequency resolution of AR spectrum estimates is better than that of FFT based spectrum estimates due to implicit extrapolation of the autocorrelation. Thus, the time-frequency resolution of the Kalman smoother spectrum is highly competent.

The adaptation of the proposed spectrum estimation method can be adjusted with a single parameter, i.e. the update coefficient UC. The decision of this coefficient should be done by compromising between the adaptation speed and the variance of the AR parameter estimates. By using the error propagation formula presented in this paper, the variance of the corresponding AR spectrum estimate can be further evaluated and thereby used in determination of UC.

Another advantage of the presented method is that the spectrum can be divided into separate frequency components. This is especially advantageous in HRV analysis, because it enables a separate estimation and investigation of the LF and HF components. The powers of these components can be estimated by directly evaluating the area of the spectral component or by using the residue based method proposed in (Johnsen and Andersen 1978).

When the component powers were compared to the corresponding band powers

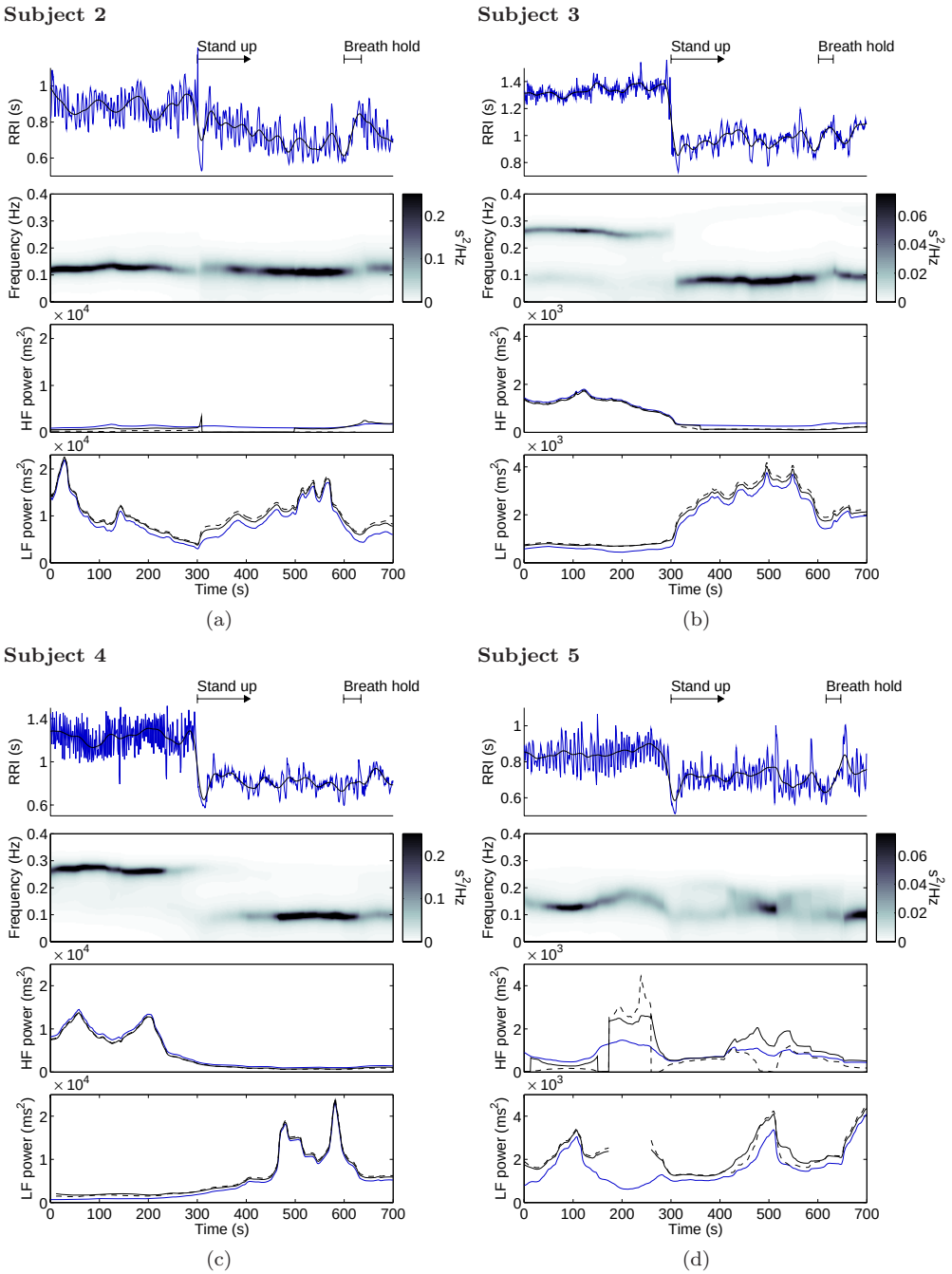

Figure 8. Time-varying spectrum estimation results for subjects 2–5. The RR interval series with the estimated trend (top), the Kalman smoother spectrum estimates (middle), and LF and HF component powers (bottom) as band powers from non-decomposed spectrum (—), areas of corresponding decomposed spectral components (—), and by using the residue method (– – –).

in figures 7 and 8, it was observed that for the LF the component powers were mostly higher than the corresponding band powers. This is mainly due the wideness of the LF component, i.e. the LF component overlaps with both the VLF and HF bands. The level of this overlap naturally depends on the central frequency of the LF component. The central frequencies of both the LF and HF components are highly individual and may also vary according to the physical circumstances. Thus, it is reasonable to argue that in some cases the LF and HF powers can be evaluated more accurately from the decomposed spectrum. The component-wise power estimation may, however, yield highly distorted results when the decomposition of the LF and HF components is not clear and, thus, this kind of power estimation should be used with care.

References

Akaike H 1969 Fitting autoregressive models for prediction *Ann. Inst. Stat.Math.* **21** 243–247

Akaike H 1974 A new look at the statistical model identification *IEEE Trans. Autom. Control* **19** 716–723

Berntson G G, Bigger Jr J T, Eckberg D L, Grossman P, Kaufmann P G, Malik M, Nagaraja H N, Porges S W, Saul J P, Stone P H and Van Der Molen M W 1997 Heart rate variability: Origins, methods, and interpretive caveats *Psychophysiology* **34** 623–648

Bianchi A M, Mainardi L, Petrucci E, Signorini M G, Mainardi M and Cerutti S 1993 Time-variant power spectrum analysis for the detection of transient episodes in HRV signal *IEEE Trans. Biomed. Eng.* **40**(2) 136–144

Bianchi A M, Mainardi L T, Meloni C, Chierchia S and Cerutti S 1997 Continuous monitoring of the sympatho-vagal balance through spectral analysis *IEEE Eng. Med. Biol. Mag.* **16**(5) 64–73

Bohlin T 1977 Analysis of EEG signals with changing spectra using a short-word Kalman estimator *Math. Biosci.* **35** 221–259

Goto S, Nakamura M and Uosaki K 1995 On-line spectral estimation of nonstationary time series based on AR model parameter estimation and order selection with a forgetting factor *IEEE Trans. Signal Process.* **43**(6) 1519–1522

Haseyama M and Kitajima H 2001 An ARMA order selection method with fuzzy reasoning *Signal Process.* **81** 1331–1335

Isaksson A and Wennberg A 1976 Spectral properties of nonstationary EEG signals, evaluated by means of Kalman filtering: Application examples from a vigilance test *Quantitative Analytic Studies in Epilepsy*, ed P Kellaway and I Petersen (Raven Press) pp 389–402

Johnsen S J and Andersen N 1978 On power estimation in maximum entropy spectral analysis *Geophysics* **43** 681–690

Keselbrener L and Akselrod S 1996 Selective discrete Fourier transform algorithm for time-frequency analysis: method and application on simulated and cardiovascular signals *IEEE Trans. Biomed. Eng.* **43**(8) 789–802

Mainardi L T and Cerutti M S 2004 Automatic decomposition of Wigner distribution and its application to heart rate variability *Methods Inf Med* **43**(1) 17–21

Marple S L 1987 *Digital Spectral Analysis* (Prentice-Hall International)

Melsa J L and Cohn D L 1978 *Decision and Estimation Theory* (McGraw-Hill)

Novak P and Novak V 1993 Time/frequency mapping of heart rate, blood pressure and respiratory signals *Med. Biol. Eng. Comput.* **31** 103–110

Pola S, Macerata A, Emdin M and Marchesi C 1996 Estimation of the power spectral density in nonstationary cardiovascular time series: assessing the role of the time-frequency representations (TFR) *IEEE Trans. Biomed. Eng.* **43**(1) 46–59

Rauch H E, Tung F and Striebel C T 1965 Maximum likelihood estimates of linear dynamic systems *AIAA Journal* **3** 1445–1450

Rissanen J 1983 A universal prior for the integers and estimation by minimum description length *Ann. Stat.* **11** 417–431

Schack B, Bareshova E, Grieszbach G and Witte H 1995 Methods of dynamic spectral analysis by self-exciting autoregressive moving average models and their application to analysing biosignals *Med. Biol. Eng. Comput.* **33** 492–498

Tarvainen M P, Hiltunen J K, Ranta-aho P O and Karjalainen P A 2004 Estimation of nonstationary EEG with Kalman smoother approach: an application to event-related synchronization (ERS) *IEEE Trans Biomed Eng* **51**(3) 516–524

Tarvainen M P, Ranta-aho P O and Karjalainen P A 2002 An advanced detrending method with application to HRV analysis *IEEE Trans. Biomed. Eng.* **49**(2) 172–175

Vila J, Palacios F, Presedo J, Fernández-Delgado M, Felix P and Barro S 1997 Time-frequency analysis of heart-rate variability *IEEE Eng. Med. Biol. Mag.* **16**(5) 119–126

Wiklund U, Akay M and Niklasson U 1997 Short-term analysis of heart-rate variability by adapted wavelet transforms *IEEE Eng. Med. Biol. Mag.* **16**(5) 113–118